10.2478/acsc-2013-0011

Archives of Control Sciences
Volume 23(LIX), 2013
No. 2, *pages 187–203*

Effects of sliding surface on the performances of adaptive sliding mode slip ratio controller for a HEV

BASANTA KUMAR DASH and BIDYADHAR SUBUDHI

Slip ratio control of a ground vehicle is an important concern for the development of antilock braking system (ABS) to avoid skidding when there is a transition of road surfaces. In the past, the slip ratio models of such vehicles were derived to implement ABS. It is found that the dynamics of the hybrid electric vehicle (HEV) is nonlinear, time varying and uncertain as the tire-road dynamics is a nonlinear function of road adhesion coefficient and wheel slip. Sliding mode control (SMC) is a robust control paradigm which has been extensively used successfully in the development of ABS of a HEV. But the SMC performance is influenced by the choice of sliding surface. This is due to the discontinuous switching of control force arising in the vicinity of the sliding surface that produces chattering. This paper presents a detailed study on the effects of different sliding surfaces on the performances of sliding mode based adaptive slip ratio control applied to a HEV.

Key words: sliding mode control, slip ratio control, hybrid electric vehicle, sliding surface, ABS

1. Introduction

Recently electric motors and electronic control system have been widely used in passenger vehicles, resulting in a significant improvement in vehicle's safety and stability. The power controller of the drive train of an electric vehicle regulates the motor current and voltage. Thus, tractive/braking control becomes fast and precise. Electric motors are excellent actuators for motion control compared to hydraulic braking systems. By using electric motor, regenerative braking together with improved antilock performance can also be achieved in HEVs [1].

The maximum tractive/braking force of a HEV that the tire-ground contact can support is determined by the normal load on the drive axle(s) and the coefficient of road adhesion which in turn depends on the wheel slip ratio and tire/road conditions.

The maximum tractive/braking effort as determined by the nonlinear nature of the tire-road interaction imposes a fundamental limit on the vehicle performance character-

B. K. Dash is with Department of Electrical Engineering, Indus College of Engineering, Bhubaneswar, BPUT, Odisha, India, e-mail: bkdash@indus.ac.in. B. Sibudhi is with Department of Electrical Engineering, National Institute of Technology, Rourkela, Odisha, India, e-mail: bidyadharnitrkl@gmail.com

Received 02.01.2013.

istics, including maximum speed and acceleration/deceleration etc. When the braking force reaches the limiting value determined by the normal load and the coefficient of road adhesion, tires are at the point of sliding. Any further increase in the braking force would cause the tires to lockup which is a major concern during braking on slippery or icy roads.

When the rear tires lockup first, the vehicle looses directional stability and the capability of the tires to resist lateral acceleration is reduced to zero [14]. The lockup of front tires will cause a loss of directional control and the driver will no longer be able to exercise effective steering.

A number of investigations have been proposed different control techniques for achieving improved braking performance of the HEVs [18] that employ electric vehicles such as fuzzy logic control [4-6], neural network control [1,7], feedback linearization control [8, 17], iterative learning control [9], and sliding mode control [1-3]. All these control approaches intended to control slip ratio accurately thereby reducing the stopping distance by preventing wheel lockup with simultaneously providing directional control and stability. Among all these control techniques used to control the slip ratio, the SMC has widely been implemented [1-3, 11-13, 15] because of its robust characteristics for nonlinear systems with model uncertainties.

In the development of SMC, the choice of the sliding surface influences the behavior of the overall control performance. Due to the discontinuous switching of control force in the vicinity of the sliding surface, it produces a chattering which can cause system instability and damage to both actuators. During the application of braking torques to the braking system, the performance of switching control may be degraded due to the braking torque limitation, brake actuator delay, and tire-force buildup, resulting in an oscillation near the sliding surface. Thus, a reduction of a chattering and a rapid convergence to the sliding surface in the actual brake systems are important. In order to reduce the chattering, a higher order SMC and a boundary- layer method with moderate tuning of a saturation function have been used in [10]. A sliding mode controller for enhancing braking performance by the control of slip ratio has been discussed in [1, 2]. When the parameters associated with HEV while moving on the road, are uncertain and time varying, the choice of an adaptive SMC to control the slip ratio of a HEV is very important which has been used in [1] but this paper does not study the effect of sliding surface design on the performance of the slip control system. It may be noted that the performance of SMC depends on the choice of proper sliding surface. However, the effects of choice of sliding surface on the overall performance (minimizing chattering, improving the tracking speed, error convergence etc.) have not been extensively investigated in slip ratio control except some limited research in [11, 15]. The effect of sliding surface design on the performance of SMC based antilock braking system has been presented in [15], but the SMC in this paper is not adaptive. Hence, this paper focuses on the study of effect of sliding surface design for adaptive sliding mode controller applied to control the slip ratio of a HEV.

The rest of the paper is organized as follows. The slip ratio model of the HEV is described in section 2. Section 3 presents problem statement for the slip ratio control.

An adaptive SMC applied to the slip ratio control of the HEV is discussed for different sliding surfaces and their effects on control performance are presented in section 4. Section 5 presents results and discussions. Finally, conclusions are provided in section 6.

2. Slip ratio model of the HEV

A good schematic model as well as a mathematical model of a ground vehicle to represent its dynamic model is essentially a prerequisite for designing controllers such as slip ratio control which will be used for analysis, design of controllers and computer simulations.

Slip is defined as the difference between the vehicle and wheel speeds, normalized by the maximum of these velocity values. Mathematically, slip ratio is defined as

$$\lambda = \frac{\omega_w - \omega_v}{\max(\omega_w, \omega_v)} \tag{1}$$

where ω_v and ω_w are vehicle and wheel angular velocity respectively. The relationship between the linear and angular velocities of the vehicle is

$$v = r_w \omega_v \tag{2}$$

Wheel speed is greater than vehicle speed in case of acceleration and vice versa in case of braking. To design a slip ratio controller, the system dynamic equation has to be represented in terms of the wheel slip and the state variables.

Choosing $x_1 = \omega_v$ and $x_2 = \omega_w$ as two state variables, equation (1) can be rewritten as

$$\lambda = \frac{x_2 - x_1}{\max(x_1, x_2)} \tag{3}$$

Fig.1 shows the vehicle wheel model during a braking mode. T_b is the braking/traction torque, ω_w is the wheel angular velocity of the vehicle, υ is the linear velocity of the vehicle, m is the mass of the vehicle and g is the acceleration due to gravity and f_b is the braking force.

When T_b is applied to the tire, a corresponding f_b is developed on the tire-ground contact patch which is the primary retarding force as shown in Fig.1. This braking effort f_b has a moment $f_b r_w$.

When the braking force is below the limit of tire-road adhesion, it is given by

$$f_b = \frac{T_b - \sum J_w \dot{\omega}_w}{r_w} \tag{4}$$

The maximum braking force that the tire-ground contact can support is determined by the normal load and the coefficient of road adhesion.

$$f_{b\,\max} = \mu(\lambda) F_N = \mu(mg) \tag{5}$$

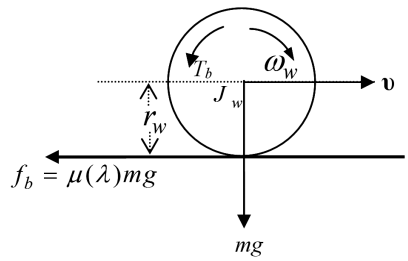

Figure 1. Wheel dynamics during braking of a quarter vehicle model.

where μ is the coefficient of road adhesion and is a function of slip (λ) and F_N is the normal tire reaction force depends on vehicle parameters such as mass, location of center of gravity and the steering and suspension dynamics. The adhesion coefficient μ is the ratio between the tire tractive force and the normal load, depends on the tire-road contact and the value of wheel slip (λ) and can be written as [1]

$$\mu(\lambda) = \frac{2\mu_p\lambda_p\lambda}{\lambda_p{}^2 + \lambda^2} \tag{6}$$

where μ_p and λ_p are the peak values. Equation (6) is compatible with experimental data in the desirable range shown in Fig. 2 [14]. For various road surface conditions (dry, wet, ice), the curves have different peak values and slopes shown in Fig.2. The $(\mu - \lambda)$ characteristics also depend on operational parameters like vehicle speed and vertical load.

With four wheel brakes, the maximum braking forces on the front and rear axles are given by

$$f_{bf\,\max} = \mu W_f = \mu(m_f g), \tag{7}$$

$$f_{br\,\max} = \mu W_r = \mu(m_r g). \tag{8}$$

When the braking forces reach the values determined by the above equations (5, 7, and 8) tires are at the point of sliding. Any further increase in the braking force would cause the tires to lockup.

Fig. 3 shows the general characteristics of the braking effort coefficient and the coefficient of cornering force at a given slip angle as a function of skid for a pneumatic tire. The rotational motion of the wheel and translational motion of the vehicle can be described as follows.

When wheel is locked, $\omega_w = 0$ and $\lambda = -1$.
When wheel is in free motion, $\omega_w = \omega_v$ and $\lambda = 0$.
The slip has a maximum value 1. The possible range of slip is $-1 \leqslant \lambda \leqslant 1$.

Slip ratio λ is a function of vehicle speed and wheel speed. Vehicle speed is a function of f_b. Wheel speed is a function of T_b and f_b which is unknown but related to λ.

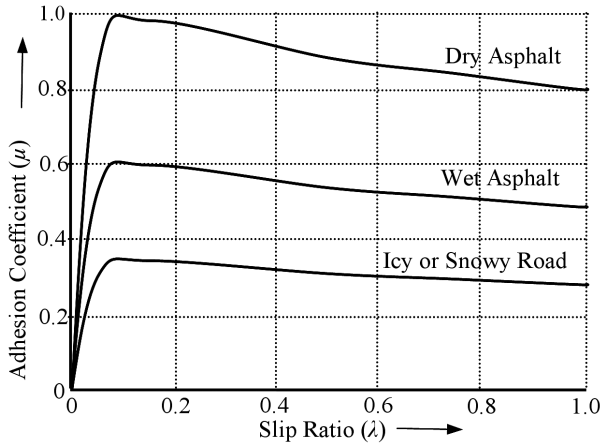

Figure 2. Typical adhesion coefficients (μ) versus slip ratio (λ) curve for different road conditions [16].

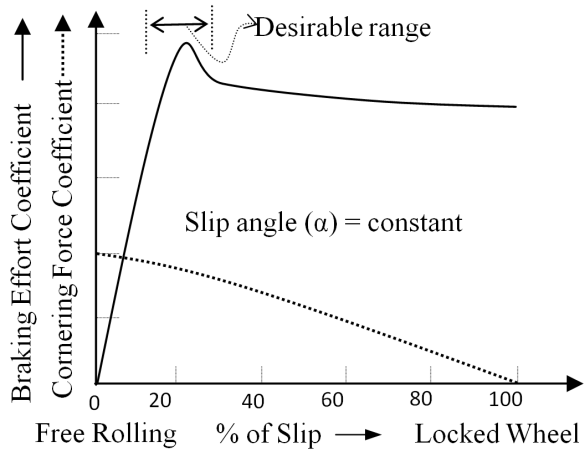

Figure 3. Effect on a skid on cornering force coefficient of a tire at a given slip angle.

The dynamics of the angular motion of the wheel and the translational motion of the vehicle can be described respectively as the following equations. The total torque consists of shaft torque which is opposed by break torque and the torque components due to tire tractive force and wheel viscous friction force. The wheel viscous friction force (f_w) developed on the tire-road contact surface depends on the wheel slip.

$$J_w\dot{\omega}_w = T_b - r_w(f_b + f_w)$$
$$J_w\dot{\omega}_w = T_b - r_w(\mu(\lambda)mg + f_w)$$

where $f_w = c\omega_w$

$$m\dot{\upsilon} = n_w\mu(\lambda)mg - c_v\upsilon^2. \tag{9}$$

Substituting (2) into (9), we have $m\dot{\omega}_v r_w = n_w\mu(\lambda)mg - c_v{\omega_v}^2{r_w}^2$

$$\dot{\omega}_v = \frac{n_w g}{r_w}\mu(\lambda) - \frac{c_v r_w}{m}{\omega_v}^2. \tag{10}$$

Again from (9), we have

$$\dot{\omega}_w = \frac{T_b}{J_w} - \frac{r_w}{J_w}\mu(\lambda)mg - \frac{r_w}{J_w}f_w. \tag{11}$$

Recalling our choice of state variables as $x_1 = \omega_v$ and $x_2 = \omega_w$ and using (10) and (11), state space representation of the slip ratio model of the vehicle can be obtained as

$$\dot{x}_1 = f_1(x_1) + c_1\mu(\lambda) \tag{12}$$

$$\dot{x}_2 = f_2(x_2) + c_2\mu(\lambda) + c_3 T_b \tag{13}$$

$$y = x_2 \tag{14}$$

where

$$f_1(x_1) = -\frac{c_v r_w}{m}{x_1}^2 \tag{15}$$

$$f_2(x_2) = -\frac{r_w f_w(x_2)}{J_w} \tag{16}$$

$$c_1 = \frac{n_w g}{r_w}, \quad c_2 = -\frac{r_w mg}{J_w} \quad \text{and} \quad c_3 = \frac{1}{J_w}. \tag{17}$$

The slip ratio model given by (12), (13) and (14) is a single-input-single-output (SISO) nonlinear system where the functions $f_1(x_1)$ and $f_2(x_2)$ are uncertain functions due to the dependence upon the road condition parameter, $\mu(\lambda)$.

A DC motor acts as an actuator which is controlled with variable armature voltage keeping the field current constant. The torque is considered to be positive during the traction, and negative during the braking. The dynamics of the actuator is described by the following equation.

$$V = \frac{L}{K_m}\frac{dT_b}{dt} + \frac{R}{K_m}T_b + K_b\omega_w \tag{18}$$

where R and L are the resistors and inductors of the armature circuit respectively.

3. Problem statement

In this paper, longitudinal vehicle motion control is considered by modeling an antilock braking system for a quarter model of a vehicle in deceleration mode for braking without cornering. For the sake of simplicity consider $x_1 > 0$ and $x_2 > 0$.

For the case of braking, $x_1 > x_2$, from (3) we have

$$\lambda = \frac{x_2 - x_1}{x_1}. \tag{19}$$

Differentiating (19) with respect to time gives

$$\dot{\lambda} x_1 + \lambda \dot{x}_1 = \dot{x}_2 - \dot{x}_1. \tag{20}$$

Substituting $\dot{x}_1$ and $\dot{x}_2$ from (12-14) in (20) yields

$$\dot{\lambda} = f(\lambda, x) + bu \tag{21}$$

where

$$f(\lambda, x) = \frac{f_2(x_2) - (1+\lambda) f_1(x_1) + [c_2 - (1+\lambda) c_1]\mu(\lambda)}{x_1} \tag{22}$$

$$u = \frac{T_b}{x_1} \tag{23}$$

$$b = c_3 \tag{24}$$

$$x = [x_1, x_2]^T. \tag{25}$$

The control gain b is unknown and assumed as constant gain with known bounds and its estimated value is $\hat{b}$ in the SMC design. Hence, development of control is based on general equation (21), where $f(\cdot)$, b, u for braking are given in equations (22-24). The adhesion coefficient $\mu(\lambda)$ can be calculated from equation (6).

The $(\mu - \lambda)$ characteristic is not exactly known and nonlinear. So the nonlinear function $f(\lambda, x)$ in (21) is assumed to be unknown. From Fig.2, Fig.3 and equation (6), it can be seen that by increasing slip, the braking force between the tire and road surface increases because of increase in μ. For a given vehicle, this amounts to maximizing the adhesion friction coefficient at the tire road surface. However, once the peak of the characteristics is reached, any further increase in slip will reduce both breaking effort and cornering force and consequently induce locking of wheel and hence skidding.

The objective is to find a control u such that a desired slip ratio is maintained keeping in pace with uncertainties encountered in the wheel parameters together with varying road conditions. The controller must be robust with respect to uncertainties in the tire characteristics and variation in the road conditions. The slip-ratio dynamics is highly uncertain and nonlinear, mainly due to the tire friction characteristics. On the other hand, fast changing in operating conditions can appear. The objective of the proposed slip control system of a vehicle is to design robust nonlinear tracking control using the slip model of the vehicle given in (12-14) with slip as the controlled variable and the torque applied to the driven wheels as the input.

4. Adaptive sliding mode controller

Schematic diagram of a slip ratio sliding mode controller is shown in Fig.4.

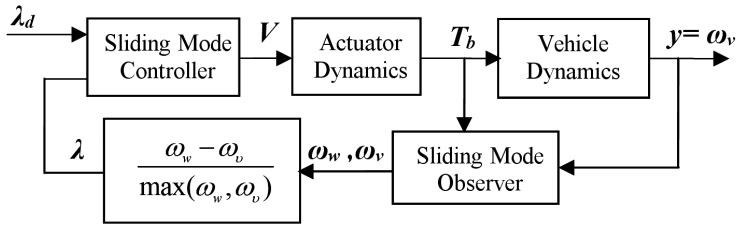

Figure 4. Structure of Slip Ratio Adaptive Sliding Mode Controller.

The SMC design procedure for controlling slip of a HEV involves three steps namely the design of the sliding surface, the design of sliding mode nonlinear observer and the design of the controller which holds the system trajectory on the sliding surface, and the chattering free implementation.

For adaptive sliding mode control design, equation (21) can be rewritten as

$$\dot{\lambda} = f_a(\lambda, x) + \theta h(\lambda, x_1) + bu \tag{26}$$

where

$$f_a(\lambda, x) = \frac{f_2(x_2) - (1+\lambda) f_1(x_1)}{x_1} \tag{27}$$

$$h(\lambda, x_1) = \frac{2[c_2 - (1+\lambda)c_1]\lambda_p \lambda}{x_1(\lambda_p{}^2 + \lambda^2)} \tag{28}$$

$$\theta = \mu_p. \tag{29}$$

The sliding mode control action is generated as follows

$$u = u_{eq} + u_d. \tag{30}$$

The equivalent control u_{eq} is given by

$$u_{eq} = \hat{b}^{-1}\hat{u} \tag{31}$$

and the discontinuous control u_d is given by

$$u_d = -\hat{b}^{-1} K \operatorname{sgn}(s). \tag{32}$$

To reduce chattering effect the discontinuous control law term, $\operatorname{sgn}(s)$ in (32) is replaced by $\operatorname{sat}(s)$ function [10] around the switching surface leading to the control

$$u = \hat{b}^{-1}\left[\hat{u} - K \operatorname{sat}\left(\frac{s}{\phi}\right)\right] \tag{33}$$

where $\phi > 0$ is the width of the boundary layer and the function of sat $\left(\frac{s}{\phi}\right)$ is defined as

$$sat\left(\frac{s}{\phi}\right) = \begin{cases} 1, & \left|\left(\frac{s}{\phi}\right) \leqslant 1\right| \\ \text{sgn}\left(\frac{s}{\phi}\right), & \left|\left(\frac{s}{\phi}\right) \geqslant 1\right| \end{cases}. \tag{34}$$

The performances of SMC are compared by defining two sliding surfaces $s(\lambda,t)$ as follows.

Sliding surface 1

$$s(\lambda,t) = \left(\frac{d}{dt} + \psi\right)^{n-1} \lambda_e \tag{35}$$

where n is the order of the system to be controlled, ψ is a positive constant, λ_e is the error which is $\lambda_e\lambda - \lambda_d$, λ_d is the desired slip. The sliding surface is

$$s(\lambda,t) = \lambda - \lambda_d, \tag{36}$$

$$\dot{s} = \dot{\lambda} - \dot{\lambda}_d. \tag{37}$$

Assuming that the desired wheel slip ratio is constant, hence,

$$\dot{\lambda}_d = 0. \tag{38}$$

On setting $\dot{s} = 0$, equation (37) gives

$$\hat{u} = -\hat{f}_a(\lambda,x) - \hat{\theta}\hat{h}(\lambda,x_1). \tag{39}$$

The control law, u can be written as

$$u = \hat{b}^{-1}\left[-\hat{f}_a(\lambda,x) - \hat{\theta}\hat{h}(\lambda,x_1) - Ksat\left(\frac{s}{\phi}\right)\right]. \tag{40}$$

$f_a(\lambda,x)$ and b are unknown. It is assumed that the nonlinear function $f_a(\lambda,x)$ can be estimated as $\hat{f}_a(\lambda,x)$, and the estimation error is assumed to be bounded by some known continuous function $F_a(\lambda,x)$, so that $\left|f_a(\lambda,x) - \hat{f}_a(\lambda,x)\right| \leqslant F_a(\lambda,x)$.

Similarly, the nonlinear function $h(\lambda,x_1)$ can be estimated as $\hat{h}(\lambda,x_1)$ and the estimation error is assumed to be bounded by some known continuous function $H(\lambda,x_1)$, so that $\left|h(\lambda,x_1) - \hat{h}(\lambda,x_1)\right| \leqslant H(\lambda,x_1)$. So we have

$$h(\lambda,x_1) \leqslant \hat{h}(\lambda,x_1) + H(\lambda,x_1). \tag{41}$$

F_a and H can be calculated using (27) and (28). Considering the uncertainty limits of the constant c_1, c_2 and c_3 to be $\pm 20\%$. $F_a(\lambda,x)$ can be thus calculated as $F_a \leqslant \left|f_a - \hat{f}_a\right|$.

Assuming the unknown control gain b is of constant sign and known bounds (a 20% bound in the estimation error can be considered), which is estimated by b, i.e.

$$0 < b_{\min} \leqslant b \leqslant b_{\max}, \quad 0 < b_{\min} \leqslant \hat{b} \leqslant b_{\max} \tag{42}$$

where

$$\hat{b} = \sqrt{(b_{\min} b_{\max})} \quad \text{and} \quad \beta^{-1} \leqslant \frac{\hat{b}}{b} \leqslant \beta \tag{43}$$

and

$$\beta = \sqrt{\frac{b_{\max}}{b_{\min}}}. \tag{44}$$

K should be chosen to satisfy the sliding condition

$$\frac{1}{2}\frac{d}{dt}s^2 \leqslant \eta\,|s| \tag{45}$$

where η is a positive constant. Thus, K can be found as

$$K \geqslant \beta(F_a + \eta + \theta_{\max} H) + (\beta - 1)\,|\hat{u}| \tag{46}$$

where $\theta_{\max}$ is the maximum value of θ. Using (46), K can be rewritten as

$$\begin{aligned} K \geqslant{}& \hat{b}b^{-1}F_a + \hat{b}b^{-1}\eta + \left|\hat{b}b^{-1} - 1\right|\left|\hat{f}_a(\lambda, x)\right| + \left|\hat{b}b^{-1} - 1\right|\left|\hat{\theta}\hat{h}(\lambda, x_1)\right| + \\ &+ \hat{b}b^{-1}(\theta_{\max} H(\lambda, x_1)). \end{aligned} \tag{47}$$

The tuning rule is chosen as [1]

$$\dot{\hat{\theta}} = \frac{\hat{h}(\lambda, x_1)s}{\gamma}. \tag{48}$$

Sliding surface 2. By adding an integral term in (35) one obtains

$$s(\lambda, t) = \lambda - \lambda_d + \int_0^t (\lambda - \lambda_d)\,dt. \tag{49}$$

Differentiating (49) and taking (38) yields

$$\dot{s} = \dot{\lambda} + \lambda - \lambda_d. \tag{50}$$

The final control law u can be written as

$$u = \hat{b}^{-1}\left[-\hat{f}_a(\lambda, x) - \hat{\theta}\hat{h}(\lambda, x_1) - \lambda + \lambda_d - K\,\mathrm{sat}\left(\frac{s}{\phi}\right)\right]. \tag{51}$$

K can be written as

$$\begin{aligned} K \geqslant{}& \hat{b}b^{-1}F_a + \hat{b}b^{-1}\eta + \hat{b}b^{-1}(\theta_{\max} H(\lambda, x_1)) + \\ &+ \left|\hat{b}b^{-1} - 1\right|\left|\hat{f}_a(\lambda, x) - \lambda + \lambda_d\right| + \left|\hat{b}b^{-1} - 1\right|\left|\hat{\theta}\hat{h}(\lambda, x_1)\right|. \end{aligned} \tag{52}$$

Table 7. HEV and actuator parameters

Torque constant (K_t)	0.2073 m-kg/amp
Back emf constant (K_b)	2.2 V/rad/sec
Inductance (L)	0.0028 H
Resistance (R)	0.125 ohm
Number of driven wheels (n_w)	4
Mass (m)	1450 kg
Moment of inertia (J)	0.65 kg m^2
Radius of the wheel (r_w)	0.31 m
Aerodynamic drag coefficient (c_v)	0.595 $N/m^2/s^2$
Desired slip ratio (λ_d)	- 0.2

5. Results and discussion

Two sliding surfaces have been selected for comparison of adaptive sliding mode controller performances for slip ratio control of a HEV and hence a simulation set up is prepared using MATLAB. The initial velocities of the vehicle and wheel are taken as 90 km/h and 89.2 km/h respectively. The braking torque is limited to 2000 Nm due the actuator limitation. The value of η, ϕ and θ are taken as 1, 0.01 and 0.3 respectively in the MATLAB simulation. The desired slip ratio is required to be -0.2 at 2.1 seconds due to change in road surface. The simulation parameters of the HEV and actuator are taken from [1] and given in Tab. 1.

For the choice of both the sliding surfaces, it can be seen from Fig. 9 and Fig. 10 that the wheel and vehicle speeds are decelerating and thus locking is avoided. The controller tracks the desired slip ratio (-0.2) perfectly for a slippery road as seen from Fig. 5 and Fig. 6. The sliding variable converges to zero which indicates that for both the cases of sliding surfaces, system states are always on the sliding plane which are shown in Fig. 7 and Fig. 8.

The response of the braking torques for both the sliding surfaces is compared in Fig. 11 and Fig. 12

After application of brake, the wheel speed suddenly falls and where as the vehicle speed slowly decreases, resulting in higher slip ratio (-0.8) and hence the wheel is in the verge of locking. But to avoid wheel locking, the wheel speed suddenly increases by the controller at 2.1 seconds to maintain the slip ratio to -0.2 shown in Fig. 9 and Fig. 10. This is done by increasing braking torque demand at 2.1 seconds by increasing the applied voltage to the actuator shown in Fig. 11, Fig. 12, Fig. 13 and Fig. 14. This phenomena relating slip ratio, braking torque, velocities and voltage requirement are true for the choice of both the sliding surface in the design of adaptive sliding mode slip

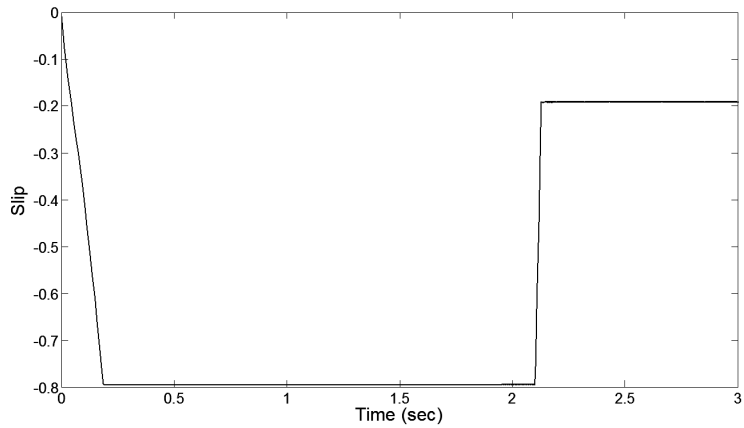

Figure 5. Slip vs time for sliding surface 1.

ratio controller. In both the cases, the controller maintains the desired slip ratio of -0.2 as shown in Fig. 5 and Fig. 6. It is noted here that while maintaining the desired slip ratio, the control activities of actuator output i.e. braking torque and actuator input i.e. required voltage have less chattering in when sliding surface 2 is chosen. This is observed from braking torque profiles (Fig. 11 and Fig. 12) and the applied voltage profile (Fig. 13 and Fig. 14). The comparison of effects of ASMC of slip ratio control of a HEV is summarized in Table 2 which shows that the chattering width in case of required braking torque and voltage requirement is reduced by 57.1% and 71.4% respectively.

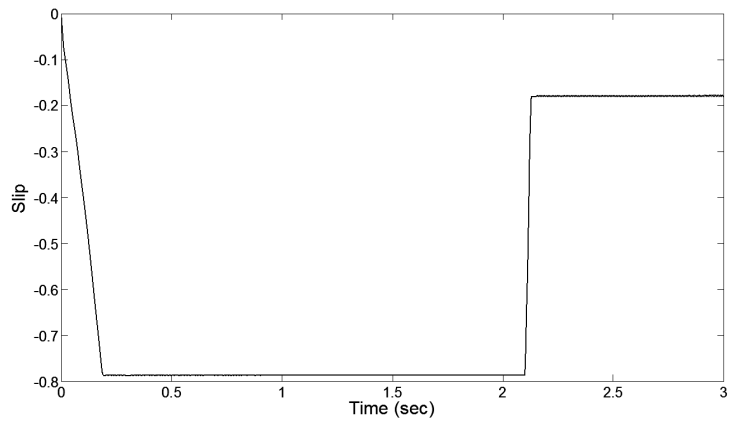

Figure 6. Slip vs time for sliding surface 2.

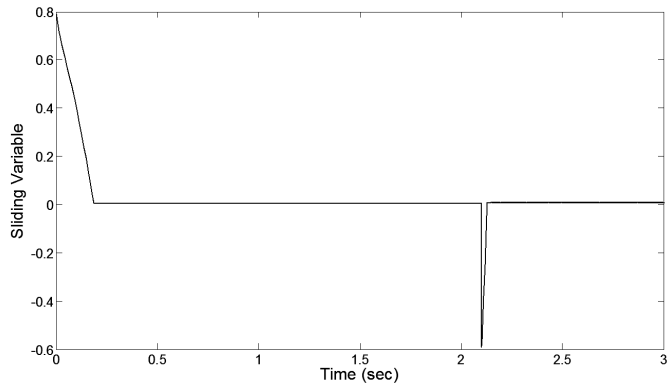

Figure 7. Sliding variable vs time for sliding surface 1.

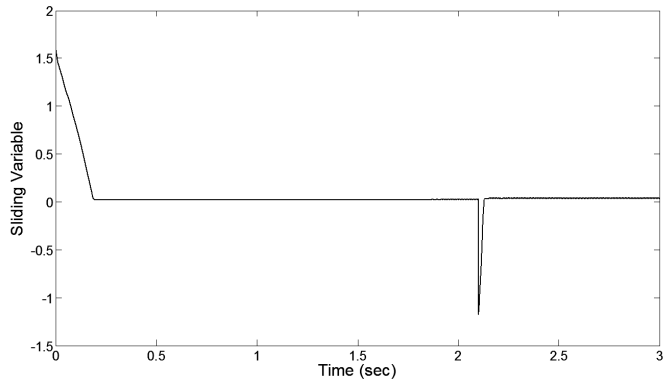

Figure 8. Sliding variable vs time for sliding surface 2.

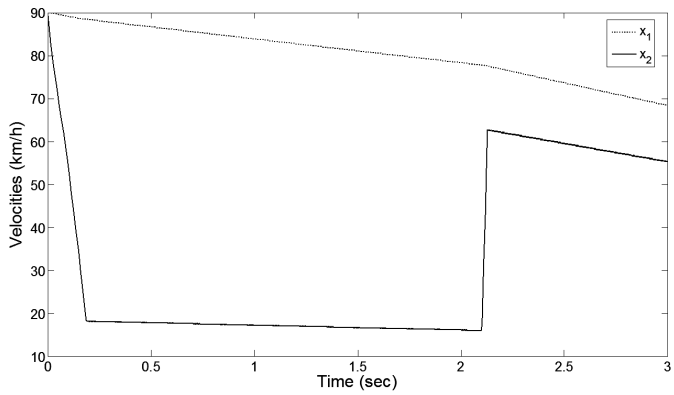

Figure 9. Velocities vs time for sliding surface 1.

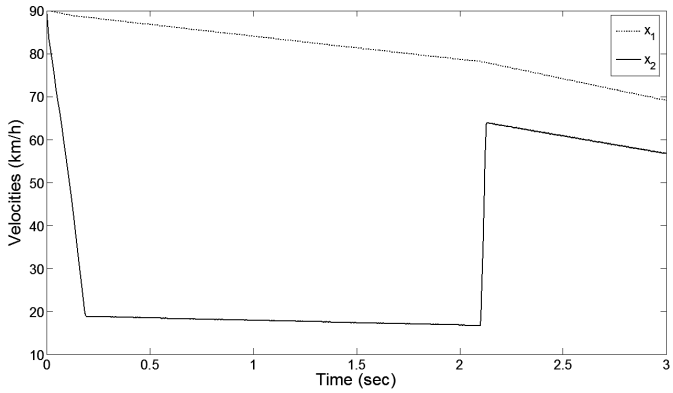

Figure 10. Velocities vs time for sliding surface 2.

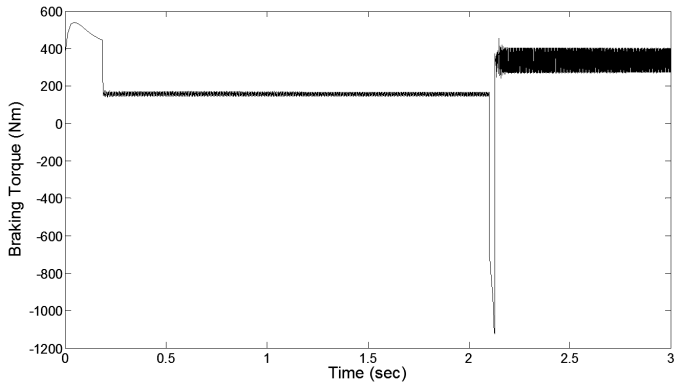

Figure 11. Braking torque vs time for sliding surface 1.

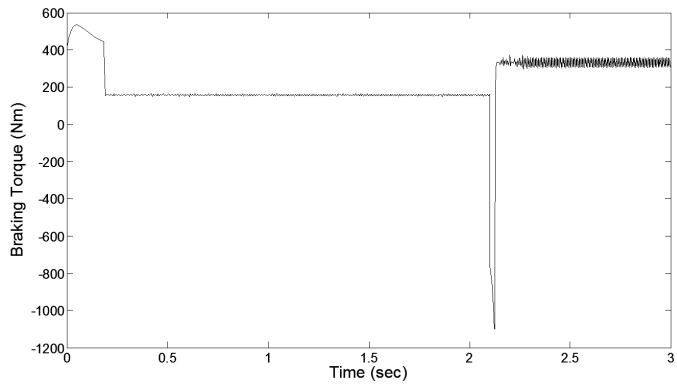

Figure 12. Braking torque vs time for sliding surface 2.

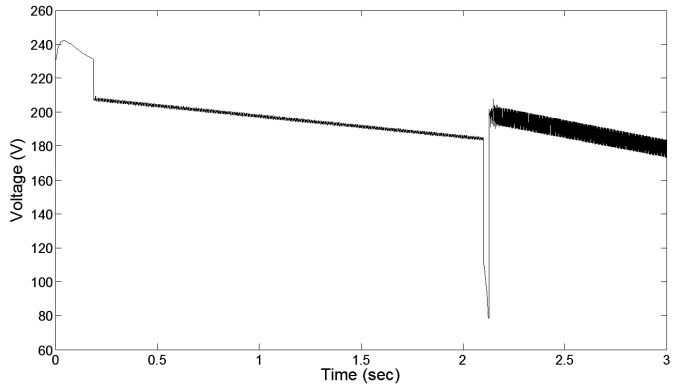

Figure 13. Required voltage vs time for sliding surface 1.

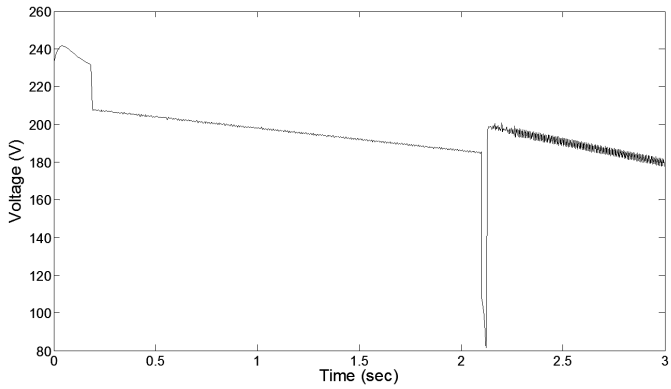

Figure 14. Required voltage vs time for sliding surface 2.

6. Conclusions

The paper has presented the design of an adaptive sliding mode slip ratio control for a HEV considering two different sliding surfaces. The controllers' parameters were tuned during on-line to track desired slip ratio of a HEV. It can be concluded from the obtained results that the choice of sliding surface having integral term for the design of adaptive sliding mode slip ratio controller for a HEV results in less chattering and less voltage requirement for tracking the desired wheel slip ratio and avoids wheel locking.

Table 8. Comparison of effects of two sliding surfaces in ASMC of slip ratio of a HEV

	Sliding surface	Braking torque (Nm)		Voltage requirement (V)	
		Chattering Amplitude	Chattering Width	Chattering Amplitude	Chattering Width
1.	$s(\lambda,t)=\lambda-\lambda_d$	260-400	140	(208-194) to (187-173)	14
2.	$s(\lambda,t)=\lambda-\lambda_d+\int_0^t(\lambda-\lambda_d)\,dt$	300-360	60	(200-196) to (178-182)	4
	Remarks	The chattering effect is less in case of sliding surface 2 in terms of amplitude, frequency and width. The chattering width is reduced by 57.1%.		The chattering effect is less in case of sliding surface 2 in terms of amplitude, frequency and width. The chattering width is reduced by 71.4%.	

References

[1] B. SUBUDHI and S.S. GE: Sliding mode observer based adaptive slip ratio control for electric and hybrid vehicles.*IEEE Trans. Intelligent Transportations*, **13**(4) (2012), 1617-1626.

[2] C. UNSAL and P. KACHROO: Sliding mode measurement feedback control for antilock braking systems. *IEEE Trans. Control Systems Technol.*, **7**(2), (1999), 271-281.

[3] K.R. BUCHHOLZ: Reference input wheel slip tracking using sliding mode control. *SAE World Congress*, Detroit, Michigan, USA, ISSN 0148-7191, (2002).

[4] J.R. LAYNE, K.M. PASSINO and S. YURKOVICH: Fuzzy learning control for antiskid braking systems. *IEEE Trans. Control Systems Technology*, **1**(2), (1993), 122-129.

[5] F. MAUER: Fuzzy learning control for antiskid braking systems. *IEEE Trans. Fuzzy Systems Technology*, **3** (1995), 381-388.

[6] P. KHATUN, C.M. BINGAM, N. SCHOFIELD and P.H. MELLOR: Application of fuzzy control algorithms for electric vehicle antilock braking/traction control systems. *IEEE Trans on Vehicular Technology*, **54**(2), (2005), 486-494.

[7] C.M. LIN and C.F. HSU: Neural network hybrid control for antilock braking systems. *IEEE Trans. Neural Networks*, **14**(2), (2003), 351-359.

[8] S. SEMMLER, R. ISERMANN, R. SCHWARZ and P. RIETH: Wheel slip control for antilock braking systems using brake-by-wire actuators. *SAE Technical Papers*, DOI: 10.4271/2003-01-0325, (2003).

[9] C. MI, H. LIN and Y. ZHANG: Iterative learning control of antilock braking of electric and hybrid vehicles. *IEEE Trans. Vehicular Technology*, **54**(2), (2005), 486-494.

[10] J.J. SLOTINE and W. LI: Applied Nonlinear Control. Prentice Hall Int. Editions, 1991.

[11] P. KACHROO and M. TOMIZUK: Integral action for chattering reduction and error convergence in sliding mode control. *American Control Conference*, Chicago, USA, (1992), 867-870. pp.867-870, June 1992.

[12] V. UTKIN: Variable structure systems with sliding modes. *IEEE Trans. on Automatic Control*, **22** (1977), 212-222.

[13] K.D. YOUNG, V. UTKIN and U. OZGUNUR: A control engineer's guide to sliding mode control. *IEEE Trans. on Control Systems Technology*, **7**(3), (1999), 328-342.

[14] J. Y. WONG: Theory of Ground Vehicles. Wiley, New York, 4th edition.

[15] T. SHIM, S. CHANG and S. LEE: Investigation of sliding-surface design of sliding mode controller in antilock braking systems. *IEEE Trans. on Vehicular Technology*, **57**(2), (2008), 747-759.

[16] B. K. DASH and B. SUBUDHI: Comparison of two controllers for directional control of a hybrid electric vehicle. *Archives of Control Sciences*, **22**(2), (2012), 125-149.

[17] O.T.C. NYANDORO J.O. PEDRO, B. DWOLATZKY and O.A. DAHUNSI: State feedback based linear slip control formulation for vehicular antilock braking system. *Proc. of the World Congress on Engineering 2011*, **I WCE** London, U.K., (2011).

[18] L. AUSTIN and D. MURREY: Recent advances in antilock braking systems and traction control systems. *Proc. of the Institute of Mechanical Engineers*, Part D: Journal of Automobile Engineering, **214** (2000), 625-638.